Control of a Multiple-Effect Falling-Film Evaporator Plant

ARTICLE *in* INDUSTRIAL & ENGINEERING CHEMISTRY RESEARCH · MARCH 2005

Impact Factor: 2.59 · DOI: 10.1021/ie049397w

2 AUTHORS, INCLUDING:

Karlene A Hoo

Montana State University

110 PUBLICATIONS **1,605** CITATIONS

Control of a Multiple-Effect Falling-Film Evaporator Plant

Z. Stefanov and K. A. Hoo*

Department of Chemical Engineering, Mail Stop 3121, Texas Tech University, Lubbock, Texas 79409-3121

This work studies the control of a single falling-film evaporator and a multiple-effect falling-film evaporator plant. The specific case studied is the concentration of solids found in the liquor that is part of the production of sulfate (kraft) pulp. The concentrated stream is the feed to the recovery boiler, a unit operation that plays a significant role in the economics of the pulp mill. The disturbance compensation of a single-loop strategy based on proportional−integral feedback controllers is compared against a model-based strategy that uses optimal control theory.

1. Introduction

Multiple-effect evaporators (MEVs) are common to industries that concentrate different products, regenerate solvents, or separate solid−liquid mixtures. In certain cases, the MEV plant must be regulated stringently to meet the high-product-purity requirements especially when the economics of the product dictate market share and the viability of the entire plant.

In this work, control studies are performed on a multiple-effect falling-film evaporator plant that is common to kraft pulp mills found in pulp and paper industries. Such evaporators play a very important role in the pulp mill chemical recovery cycle by concentrating the black liquor that is a waste product of the cooking process before it is burned in the recovery boiler. The importance of maintaining a constant solids concentration in the black liquor can be explained based on the operation of the recovery boiler.[1,2]

(1) A solids concentration that is greater than the expected value results in more efficient boiler operation. This is because the total amount of water in the liquor to be evaporated by the recovery boiler is less, thus increasing the amount of heat available for steam generation. (2) The feed stream (concentrated black liquor) to the recovery boiler is first preheated. Then, the feed stream is burned to form small droplets whose size is a function of the black liquor viscosity. Variations in the size of the droplets may lead to an appreciable decrease in the bed temperature, resulting in low recovery boiler efficiency. However, a more serious problem arises if the droplets are very small. Small droplets will exit with the flue gases, resulting in both chemical losses and an increase in the amount of fly ash. Excessive amounts of fly ash tend to block the heat-exchange surface, resulting in meltdown of the superheater tubes and eventual total boiler shutdown or destruction.[3] (3) According to the Black Liquor Recovery Boiler Advisory Committee (BLRBAC),[3] a liquor whose solids concentration is less than 0.58 kg/kg (high water content) should not be burned by the recovery boiler because of the high probability of smelt/water explosions. Smelt is a byproduct of the minerals that precipitate from the black liquor during the recovery boiler process.[3]

In some pulp mills, the variability of the solids concentration is mitigated by mixing with on-site-stored concentrated black liquor. However, there are safety and ecological incentives to reduce the amount of on-site inventories; thus, a dependence on these inventories to dampen the variations in the black liquor viscosity is not a long-term viable solution.

Because smooth and efficient operation of the recovery boiler is vital to the operation of the pulp mill, there is motivation and justification to regulate the quality of the concentrated black liquor feed, which is the product of the MEV plant.

1.1. Operational Issues. Load (throughput or feed rate changes) disturbances to the evaporators are frequent to regulate on-site weak black liquor inventories. Feed composition changes also occur when the raw materials or the cooking conditions change. Also, it is possible that steam header pressure disturbances may occur if boiler operating conditions (different steam demands, scaling, failure, etc.) change.

A reliable means to measure the black liquor solids concentration directly is to employ refractometers.[4] From practical experience, some pulp mills have reported high reliability with these sensors including consistent validation with laboratory values.

2. Single-Loop Control Strategy

Much can be learned about controlling the multiple-effect falling-film evaporator plant by first studying control of a single evaporator. A phenomenological distributed parameter model was developed and validated by Stefanov and Hoo[5] and Stefanov.[6] In this section, single-loop feedback controllers are designed and their closed-loop performance is tested and analyzed using this model.

The natural variables to be controlled are the solids concentration in the product stream and the level of the evaporator. Additional control variables may include the temperature and flow rate of the product stream. The manipulated variables are the feed, product, and cooling water stream flow rates and the steam pressure. The product stream flow rate can be used as either a manipulated or controlled variable depending on whether the evaporator operation is either on supply or on demand. The usual mode of operation for most pulp mills is on supply, meaning that all of the weak black liquor must be processed. Thus, the control studies in this work will address on-supply operations, where the controlled variables are the solids concentration of the product stream and the evaporator level.

A steady-state component balance on the solids concentration in the evaporator is given by

$$G_{in}X_{in} = G_{prod}X_{prod} \quad (1)$$

* To whom correspondence should be addressed. E-mail: khoo@coe.ttu.edu.

10.1021/ie049397w CCC: $30.25
Published on Web 03/11/2005

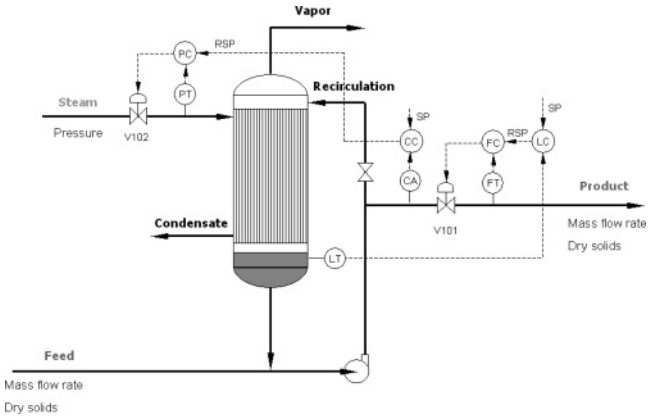

Figure 1. Single-loop feedback control strategy. There are two cascaded feedback control loops. The composition controller (CC) uses steam to regulate the solids concentration in the product stream, and the level controller (LC) uses the product stream flow rate to regulate the evaporator level.

where G_{in} and G_{prod} are the inlet and outlet mass flow rates, respectively, and X_{in} and X_{prod} are the inlet and outlet solids concentrations, respectively. Because X_{in} is a disturbance variable and G_{in} is fixed at a specified rate, neither G_{prod} nor X_{prod} can be controlled independently.

Changes in the temperature of the product stream (T_{prod}) do not affect the recovery boiler operation to the same degree as changes in the solids concentration of the product stream because the temperature of this stream is preheated by steam prior to entering the recovery boiler.

Part of any control strategy is to decide on how to pair the selected controlled and manipulated variables. One popular technique is to apply a relative gain array (RGA) analysis. Following the procedure provided in ref 7, the RGA matrix for the input steam pressure (P_s) and product stream rate (G_{prod}) and the output product stream solids concentration (X_{prod}) and evaporator level (L) is given by

$$\Lambda = \begin{bmatrix} \lambda_{X/G} & \lambda_{L/G} \\ \lambda_{X/P_s} & \lambda_{L/P_s} \end{bmatrix} = \begin{bmatrix} -0.1936 & 1.1936 \\ 1.1936 & -0.1936 \end{bmatrix} \quad (2)$$

Thus, the recommendation of the RGA analysis is to pair X with P_s and L with G. The values of the process variables for which the RGA matrix is valid are listed in Table 2. The level of the evaporator inventory is 1 m.

A schematic of the process and the proposed control strategy is shown in Figure 1.

The scheme shows two cascade feedback control loops. The introduction of the cascade structure is necessary to ensure proper disturbance rejection. Disturbances in the steam pressure can result from changes in the steam header, and disturbances in the product stream flow rate can result from variations in the recirculation pump head. Cascade feedback control loops are commonly used in many industries; what must be guaranteed for these interconnected loops to function correctly is that the time constant of the inner loop must be much faster that the time constant of the outer loop.

Actuators such as control valves do not respond immediately to the controller's command. To account for the delay in the response, the dynamics of the steam (V102) and product flow (V101) valves are modeled as first-order responses with time constants of 90 and 45 s, respectively. The control law selected is proportional–integral (PI), where the controller gain and reset time are tuning parameters. There are many methods to determine the values of the PI controller tuning parameters. In the present work, these parameters are found using the procedures given in ref 7 (Chapter 13, pp 298–309). Table 1 lists the parameter values for each PI controller. All sensor time constants are neglected.

Table 1. Single-Loop Control Parameters

loop	gain	reset time (s)	time constant (s)
FC: flow control	0.09 s·%/kg	3.3	58
FC: flow control	0.09 s·%/kg	3.3	58
PC: pressure control	0.000 09%/Pa	3.3	131
FC: flow control	0.09 s·%/kg	3.3	58
LC: level control	−368 kg/s·m	100	435
CC: composition control	1 250 000 Pa	33.3	722

2.1. Performance Evaluation. The performance of the closed-loop system is evaluated in the presence of ±5% changes in the feed mass flow rate and the feed solids concentration, a 6.2% decrease in the feed temperature, and a 10% increase in the product stream solids concentration set point. The nominal values of the process are listed in Table 2.

The simulated closed-loop responses are shown in Figure 2. The criteria for satisfactory closed-loop response include the length of time it takes the controller to return the value of the controlled variable to within $\pm 1\sigma$ of the set point, the oscillation period, the type of response, and the time to settle to the desired value. In this study, the standard deviation, σ, of for the solids concentration is 0.001 kg/kg. This value represents the error of the refractometer. From Figure 2, it is observed that all of the responses are stable and smooth and the product stream solids concentration is within the $\pm 1\sigma$ limit very quickly (3.85 min). The changes in the manipulated variables (not shown) are smooth and do not violate any constraints.

Although the PI loops are tuned for disturbance compensation, this control strategy is tested under servo control conditions, i.e., higher (10%) product solids concentrations. The cascade feedback control strategy with the tuning parameters listed in Table 1 did not produce a satisfactory performance under servo control conditions. There are at least two possible reasons for this response. First, the controller parameters (gain and reset time) should be changed and, second, the set-point change in the product stream solids concentration was in the form of a perfect step function, which may not be achievable for this or any real, nonlinear, multivariable process.

Another limitation of the cascade feedback control strategy is the inability to incorporate input and output constraints explicitly in the calculation of the controller action. Thus, there is motivation to seek a more advanced control strategy that may address some of these limitations.

3. Model-Based Control

Model-based controllers require a model of the process to determine the control action. The specific model-based controller that is developed in this work belongs to the class of model predictive controllers (MPCs). In this class of controllers, the control actions are determined at the current sample time k and $k + 1$, $k + 2$, ..., P

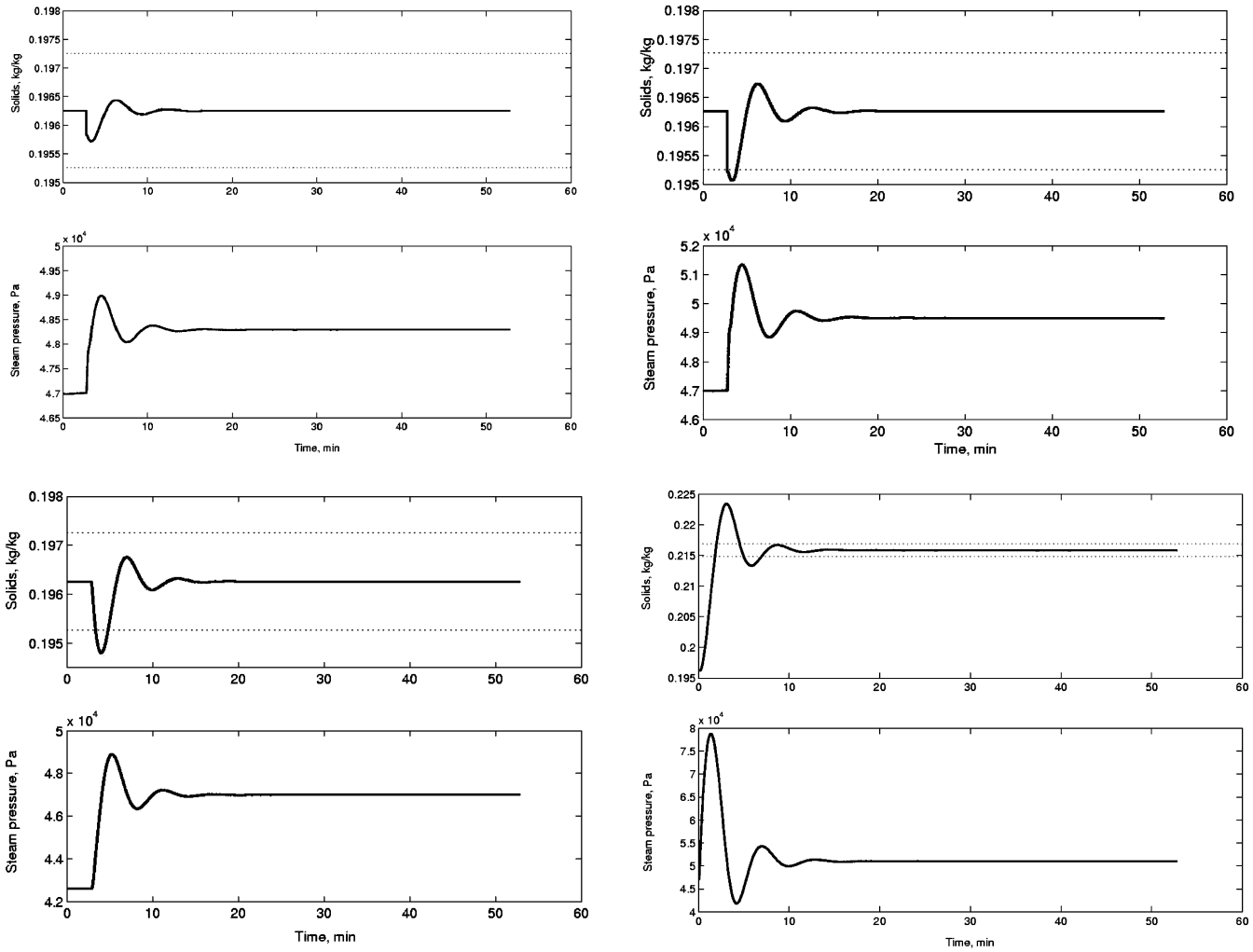

Figure 2. Closed-loop performance of the single-loop strategy of a single evaporator. Top left: a 5% increase in the feed flow rate. Top right: 5% decrease in the feed solids concentration. Bottom left: 5% decrease in the feed temperature. Bottom right: 10% increase in the set point of the solids concentration in the product stream. The dotted lines represent the $\pm 1\sigma$ limit of 0.001 kg/kg solids.

Table 2. Nominal Operating Conditions of the Single Evaporator

variable	value	variable	value
feed mass flow rate, G_f	58 kg/s	plate inventory mass	3108 kg
feed solids, X_f	0.145 kg/kg	plate inventory solids	0.2248 kg/kg
feed temperature, T_f	303.15 K	inventory solids	0.2248 kg/kg
vapor pressure, P_{vap}	24 000 Pa	inventory temperature	339.26 K
steam pressure, P_s	47 000 Pa		

steps into the future and they are optimal in the least-squares sense. One of the most important aspects of the MPC formulation is the explicit handling of constraints on the outputs (controlled variables), the inputs (manipulated variables), and the rate of change of the inputs. MPC also addresses multivariable interactions and nonminimum phase behavior. The reader is referred to the technical literature.[8]

Model fidelity is a key factor in the successful implementation of the MPC. The model can be in either a state-space form [system of continuous (discrete) differential (difference) equations] or a convolution form (input/output step or impulse models). Stefanov and Hoo[5,9] and Stefanov[6] developed and validated a fundamental distributed parameter model of a single falling-film evaporator consisting of a system of nonlinear partial differential equations (PDEs). Such a model cannot be used in the MPC framework; thus, an approximate model consisting of a system of nonlinear ordinary differential equations (ODEs) is derived and used to develop the MPC.

The nonlinear ODE (NLODE) model is developed using first principles knowledge that governs the physicochemical phenomena of the process but neglects the spatial variations (see the appendix). Figure 3 shows the responses of the NLODE and the nonlinear PDE models to changes in the feed flow rate, solids concentration, temperature, and vapor pressure. All levels are regulated by PI controllers and are omitted. It is observed that the NLODE model represents the main features of the nonlinear PDE model satisfactorily, with the process temperature responses showing the largest deviations. Additionally, the steady-state gains obtained from a ratio of the change in the outputs to the change in the inputs are equivalent.

Because the theoretical underpinnings of closed-loop stability with MPC are established for linear models, the NLODE model is approximated by a linear time-

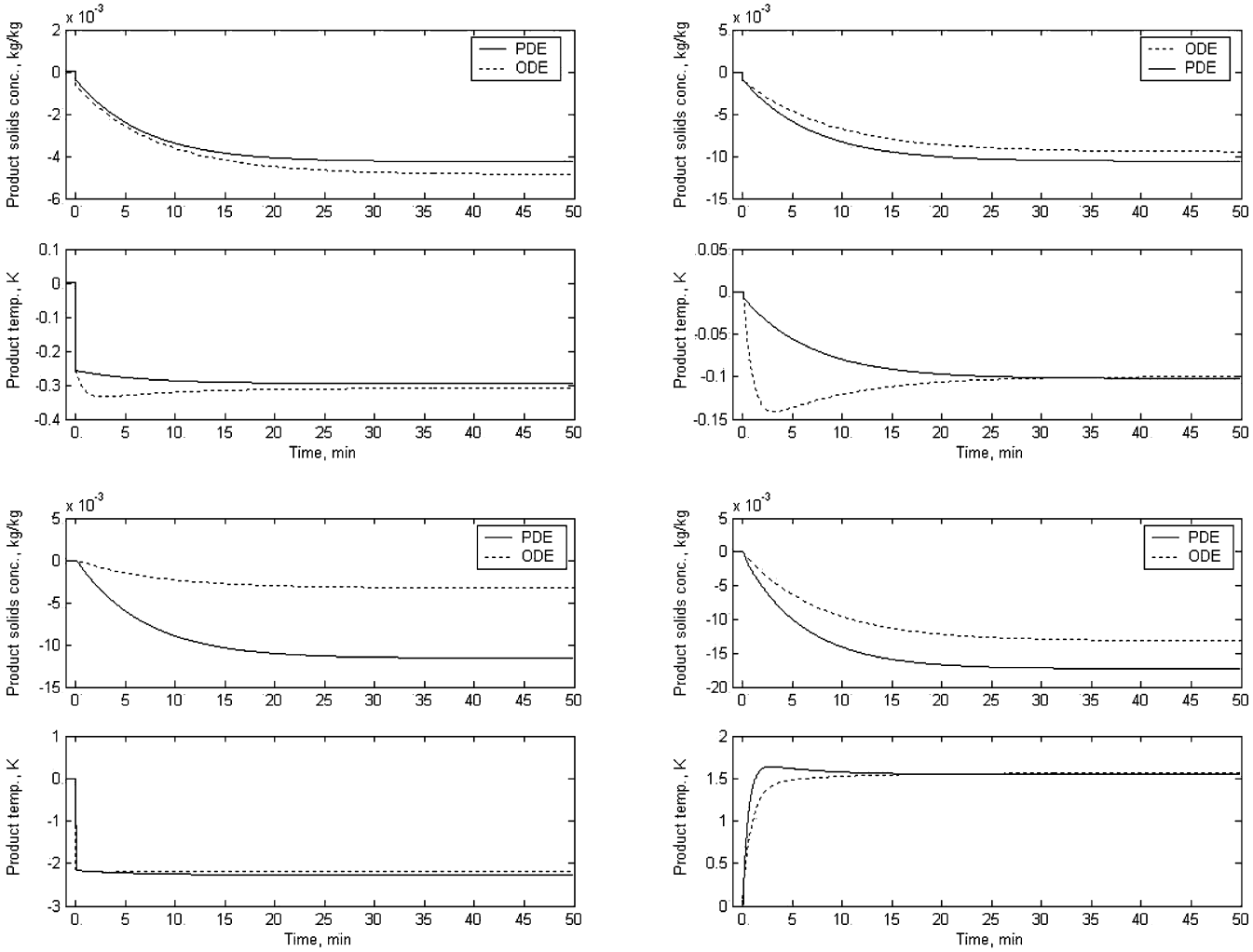

Figure 3. Validation of the NLODE model of a single evaporator. Top left: 5% increase in the feed flow rate. Top right: 5% decrease in the feed solids concentration. Bottom left: 5% decrease in the feed temperature. Bottom right: 5% increase in the vapor pressure.

invariant (LTI) model by applying a Taylor series expansion about a stable, nominal state ($\mathbf{x}_s$, $\mathbf{u}_s$). The state-space form of the LTI model is necessarily a deviation model whose form is given by

$$\frac{d\Delta\mathbf{x}}{dt} = \mathbf{A}\Delta\mathbf{x} + \mathbf{b}\Delta\mathbf{u}\Delta\mathbf{x}_0 = \mathbf{x}(0) \tag{3}$$

where $\Delta\mathbf{x}$ ($= \mathbf{x} - \mathbf{x}_s$) represents the states of the system, $\Delta\mathbf{u}$ ($= \mathbf{u} - \mathbf{u}_s$) are the inputs, $\Delta\mathbf{x}_0$ are the initial conditions, and **A** and **b** are constant coefficient arrays that represent the Jacobians with respect to the states and inputs, respectively. The output or measurement equation is given by

$$\Delta\mathbf{y} = \mathbf{C}\Delta\mathbf{x} + \mathbf{D}\Delta\mathbf{u} \tag{4}$$

where $\Delta\mathbf{y}$ are the outputs and **C** and **D** are arrays of appropriate dimension. The initial condition vector, $\Delta\mathbf{x}(0)$, is the zero vector because the model is based on deviation variables.

3.1. Model Validation. The LTI model has four states: (1) the total mass of the black liquor on the plates, (2) the solids concentration in the plate stack, (3) the solids concentration in the evaporator inventory, and (4) the temperature in the evaporator inventory (see Table 2).

A systems-theoretic analysis of the LTI model shows that the eigenvalues of the dynamic matrix **A** are real and negative.[10] Therefore, the LTI model is open-loop stable. The state and output controllability matrices are both full rank; therefore, the LTI model is state and output controllable.[11,12] The rank of the observability matrix is also full; therefore, the LTI model is observable.

Figure 4 compares the open-loop responses between the nonlinear and linear models to ±5% changes in the vapor and steam pressures. It can be concluded that the LTI model represents the nonlinear system dynamics satisfactorily because the responses are qualitatively the same and the differences in the steady-state gains are small.

3.2. Model-Based Controller Performance. The development of the MPC applied to the evaporator is accomplished using Matlab (The Mathworks, Inc., Natick, MA) and associated toolboxes. The measured (controlled) variables, expressed as deviations from their nominal values, are the solids concentration (X_{prod}) and temperature (T_{prod}) of the product stream.

The inputs, also expressed as deviation variables, are the steam (T_s) and saturation (T_v) temperatures of the process fluid. In the MPC implementation, MPC is configured as part of a supervisory control layer rather than as a part of the regulatory layer. Thus, these temperatures translate to set points on the steam (P_s) and vapor (P_v) pressures. A block diagram of the model-based control design is shown in Figure 5.

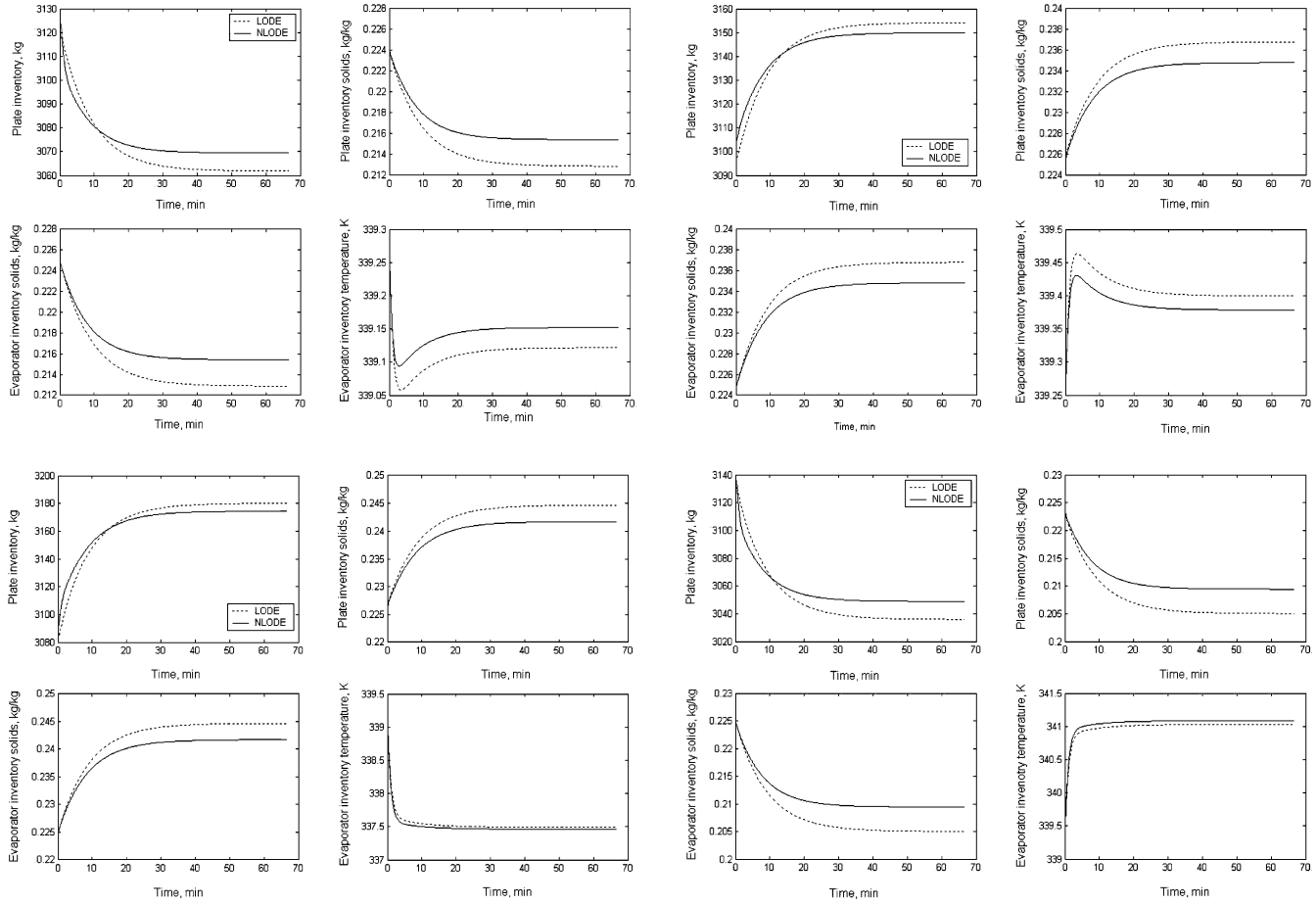

Figure 4. Validation of the LODE model of a single evaporator. Top left: 5% decrease in the steam pressure. Top right: 5% increase in the steam pressure. Bottom left: 5% decrease in the vapor pressure. Bottom right: 5% increase in the vapor pressure.

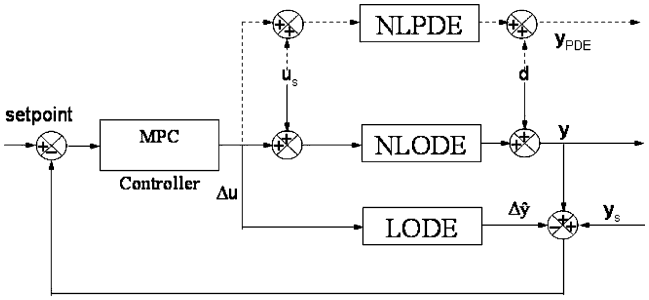

Figure 5. Block diagram of the MPC supervisory structure. The LODE model (LODE) is used by the MPC to predict the controller actions based on measurements taken from the NLODE model. The calculated controller actions are applied to regulate the nonlinear plant (NLPDE).

In the proposed controller design, it is assumed that the NLODE model is a satisfactory representation of the nonlinear PDE model. The control actions are found in response to disturbances that are introduced to both the NLODE model and the nonlinear PDE plant.

The tuning parameters of the MPC design are as follows: prediction horizon of 75 min and control horizon of 2.5 min; weights of 50 and 0.01 on X_{prod} and T_{prod}, respectively; equal weighting (0.06) on all inputs. Constraints on the outputs are as follows: -0.001 kg/kg $< X_{prod} < 0.001$ kg/kg; -0.2 K $< T_{prod} < 0.2$ K. Constraints on the inputs are as follows: -10.96 K $< T_s < 6.04$ K; -18.23 K $< T_v < 4.77$ K. Constraints on the rate of change on the inputs: ΔT_s and $\Delta T_v < 3$ K.

A single-loop feedback control strategy, similar to that presented in section 2, is developed to regulate the NLODE model of the evaporator. The tuning parameters of the PI controllers are composition and temperature loop gains/reset times of 2000 K/500 s and 30/300 s, respectively. The design parameters of either the MPCs or PI controllers are not optimal; rather, they are selected to provide satisfactory disturbance compensation.

The $\pm 1\sigma$ limits for X_{prod} and T_{prod} are ± 0.001 kg/kg and ± 0.2 K, respectively. These limits are based on expected errors associated with the analyzer or the sensor. All disturbances are modeled as step functions.

Disturbances of $\pm 5\%$ in the feed solids composition, flow rate, and temperature are applied to the evaporator process. Figures 6 and 7 compare the closed-loop performances of both controllers applied to regulate the NLODE model of the evaporator. Satisfactory disturbance compensation can be observed. In each case, the responses are smooth and without excessive overshoots or oscillations. The controller actions do not exhibit aggressive moves. All disturbances are compensated for within $\sim$35 min after the introduction of the disturbance. However, there are noticeable differences in the closed-loop responses between the two controller designs.

The PI controllers appear to provide tighter control. This is attributed to the tuning parameters selected for the PI controllers, which are unaltered for each disturbance. It is observed that the changes in the controller actions are more aggressive for all disturbance compensations.

To examine the robustness of the PI controllers and MPCs, the magnitudes of the set of disturbances are

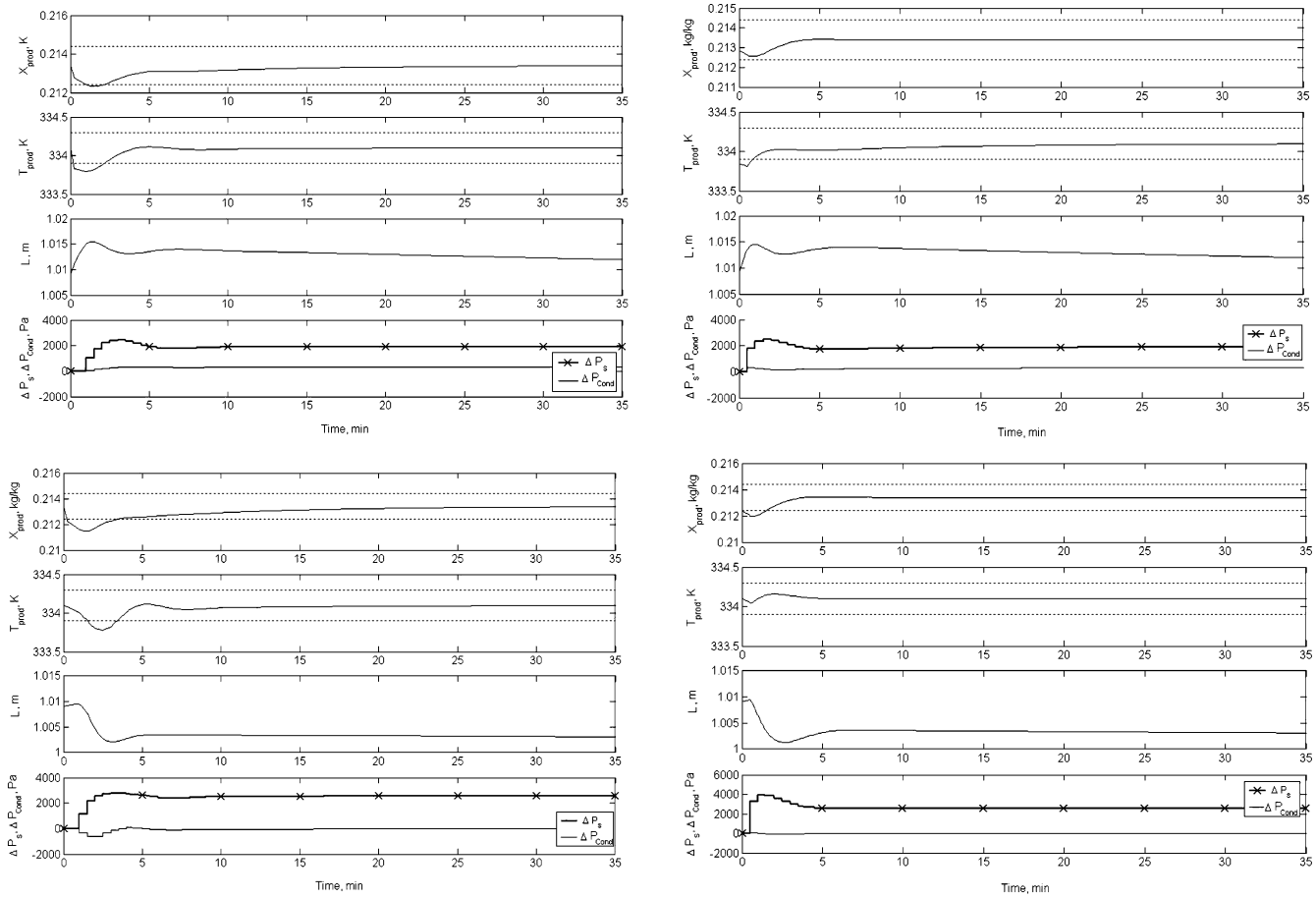

Figure 6. Disturbance compensation of the single evaporator (NLODE) with either supervisory MPCs (left) or PI controllers (right). Top: 5% increase in the feed mass flow rate. Bottom: 5% decrease in the solids concentration of the feed. The dotted lines represent the 1σ limits.

further increased by 1.6%. This increase led to input constraint violations by the PI composition controller. Thus, the parameters of this controller are changed to a gain of 1000 K (reduction by 100%) and an integral time constant of 250 s (reduction by 50%). For disturbances in the feed stream flow rate and solids concentration, no significant differences between the closed-loop responses are observed (responses are not shown). However, in the case of the feed temperature disturbance, the closed-loop responses of the MPC and PI controller strategies are dissimilar (see the bottom graphs in Figure 7).

The performance of the PI controller in the presence of the additional 1.6% increase in the feed temperature is worse when compared to that of the MPC. For instance, the time for complete compensation (time to drive the controlled variable to within $\pm1\sigma$) is about 4 times longer (20 min) in comparison to that achieved by the MPC (5 min). Figure 7 also shows that the MPC regulates well the most important variable, X_{prod}, to within $\pm1\sigma$. If the PI controllers are tuned to achieve the same performance with respect to the outputs, they may violate the rate of change limits on the input variables.

3.3. MPC of the PDE Model of the Single Evaporator. Because the MPC is successful in regulating the NLODE model of the evaporator, the optimal controller actions are applied to control the plant (nonlinear distributed parameter PDE model of the evaporator). The plant response in the presence of a 5% decrease in the feed temperature is shown in Figure 8. It is observed that X_{prod} is regulated well within $\pm1\sigma$ limits. The response of T_{prod} is not as accurate; the error is $\sim$1 K. It can be concluded that the approach to designing a linear MPC derived from a nonlinear fundamental model is satisfactory in this specific case, but no generalization can be made for other systems.

3.4. Economic Benefits. The economic benefits of applying MPC to regulate the product stream solid concentration are difficult to quantify when only one evaporator is considered. In reality, a pulp mill uses an evaporator plant (more than one evaporator) to concentrate the feed to the recovery boiler. If the solids concentration in the product stream of the MEV plant is regulated, it is possible to quantify the economic benefits of maintaining a constant solids concentration in the feed stream to the recovery boiler.

Information found in ref 13 provides an estimate of the difference in net losses/gains per year if a solids concentration between 0.75 and 0.8 kg/kg is produced by the evaporator plant as compared to a solids concentration of 0.48 kg/kg. The difference between the net loss/gain is approximately \$600 000/year. If 0.8 kg/kg is assumed to be the desired operating point and the process is maintained within $\pm1\sigma$ for 80% of the processing time but deviates within 0.01 kg/kg for the rest of the processing time, this will result in a loss of \$24 000/year. However, if 80% of the time the specification is outside $\pm1\sigma$, then for the same operating point, the loss increases up to \$96 000/year, or an increase in losses by 400%. This analysis includes only pure energy balance effects on the recovery boiler.

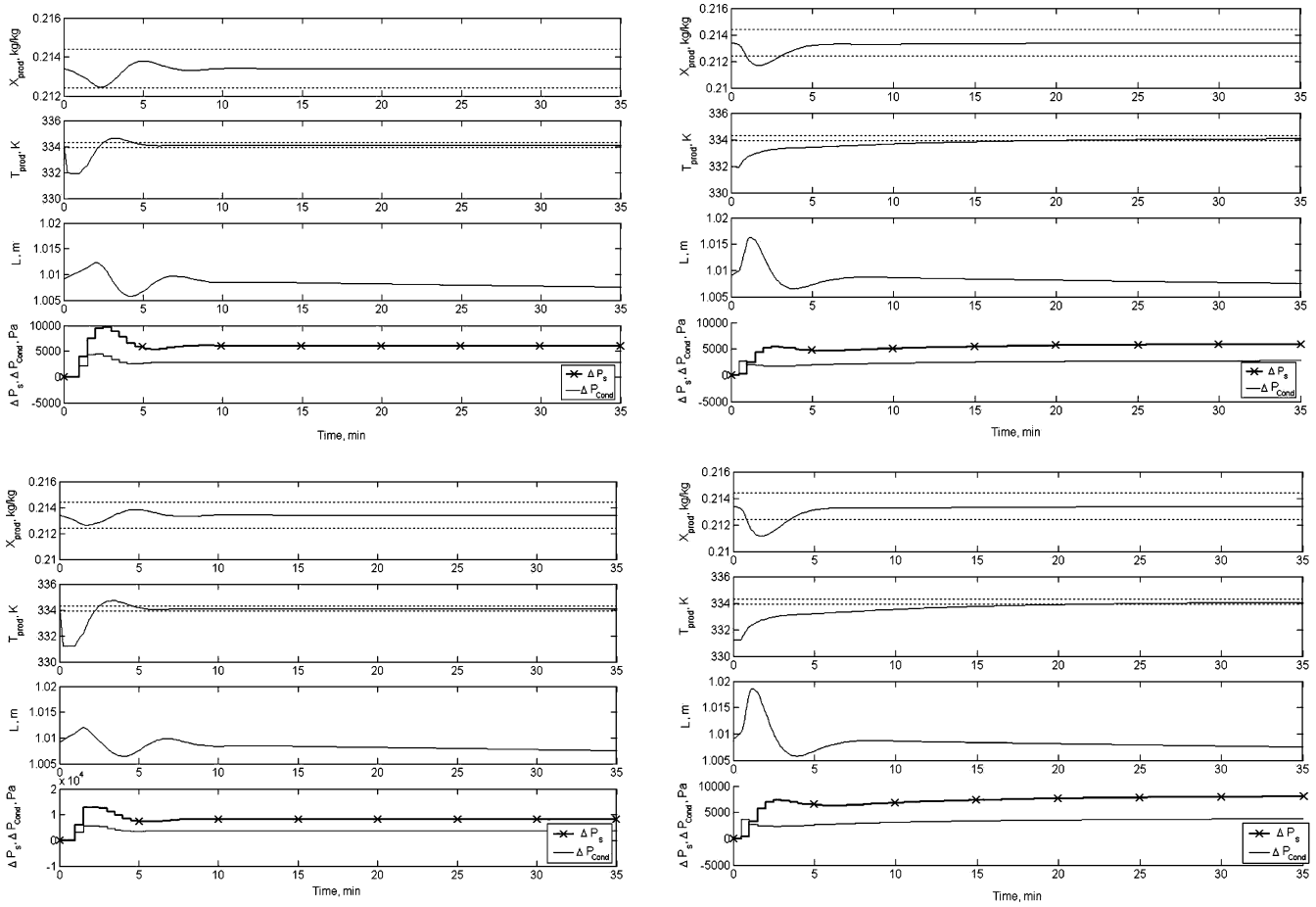

Figure 7. Robustness of the supervisory MPCs (left) and PI controllers (right) to feed temperature disturbances. Top: 5% decrease. Bottom: 6.6% decrease. The dotted lines represent the $\pm 1\sigma$ limits.

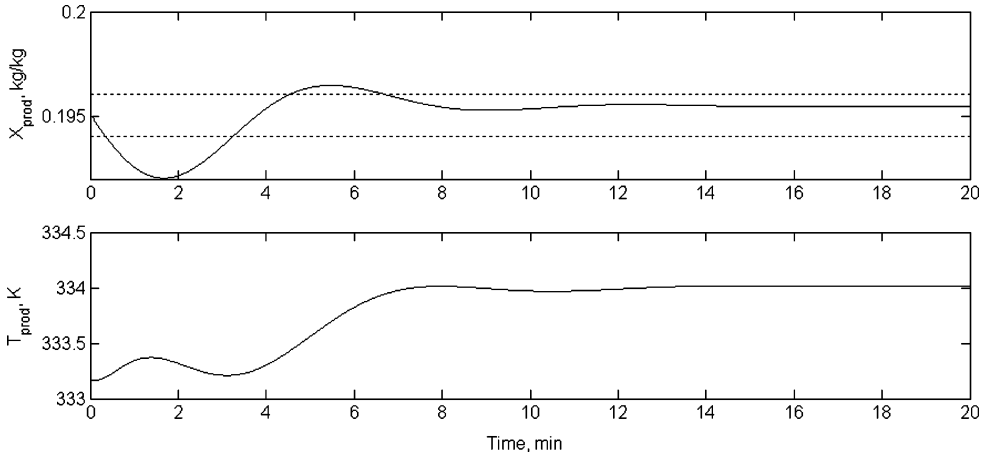

Figure 8. Control strategy validation using the nonlinear PDE model of a single evaporator. The MPC/NLODE-generated optimal control actions to a 5% decrease in the feed temperature are applied. The dotted lines represent the $\pm 1\sigma$ limits.

4. MEV Plant

The MEV plant studied in this work consists of seven evaporators, including a superconcentrator [three falling-film evaporators (SC-1−SC-3) mounted in a single body]. Figure 9 is a schematic of the plant.

4.1. Model Validation. A fundamental distributed parameter model (system of PDEs) of the MEV can be found in refs 5 and 6. Following the development provided in section 3, the NLODE model provided in ref 5 will be used to develop the MPC. Figure 10 compares the responses of the nonlinear PDE and NLODE models of evaporator 5 (E-5) and evaporator SC-1 to changes in the operating conditions. Before the changes are introduced, the evaporator levels must be regulated because they are integrating elements. The levels of E-2−E-5 are regulated by their respective effluent streams. The product stream flow rate of evaporator SC-1 is used to control the levels in the superconcentrator.

The responses show that the NLODE and nonlinear PDE models have similar trends. The profiles of the respective product stream solids concentration are similar, and the steady-state gains are on the same order. The responses to feed temperature disturbances

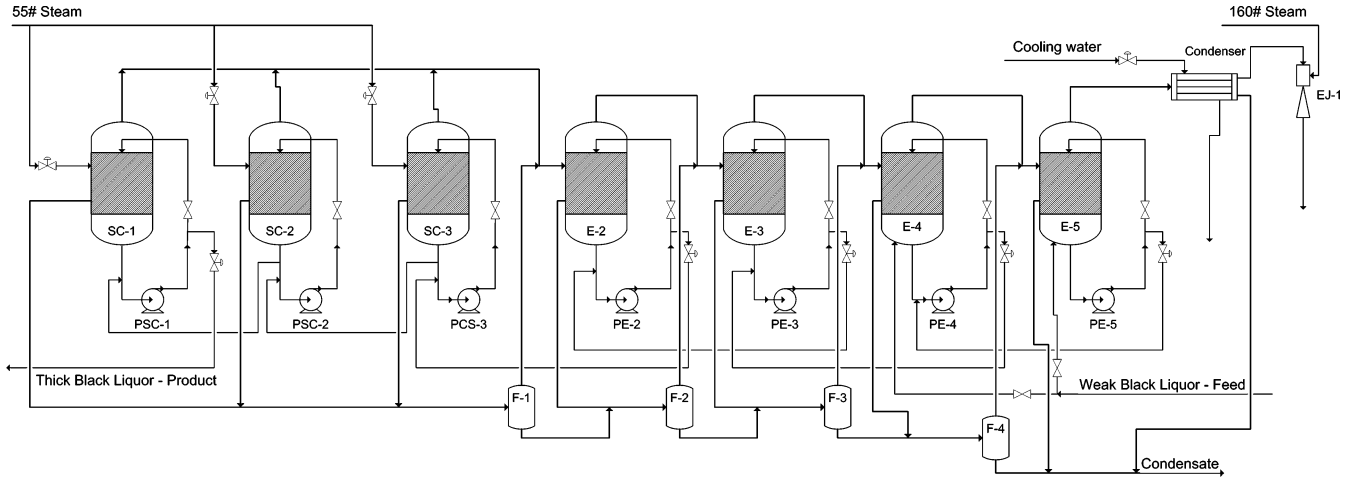

Figure 9. Multiple-effect falling-film evaporator plant. There are four evaporators, EC-2−EC-5, and one superconcentrator that contains three evaporators, SC-1−SC-3. The feed stream enters at EC-5, and the product stream exits at SC-1.

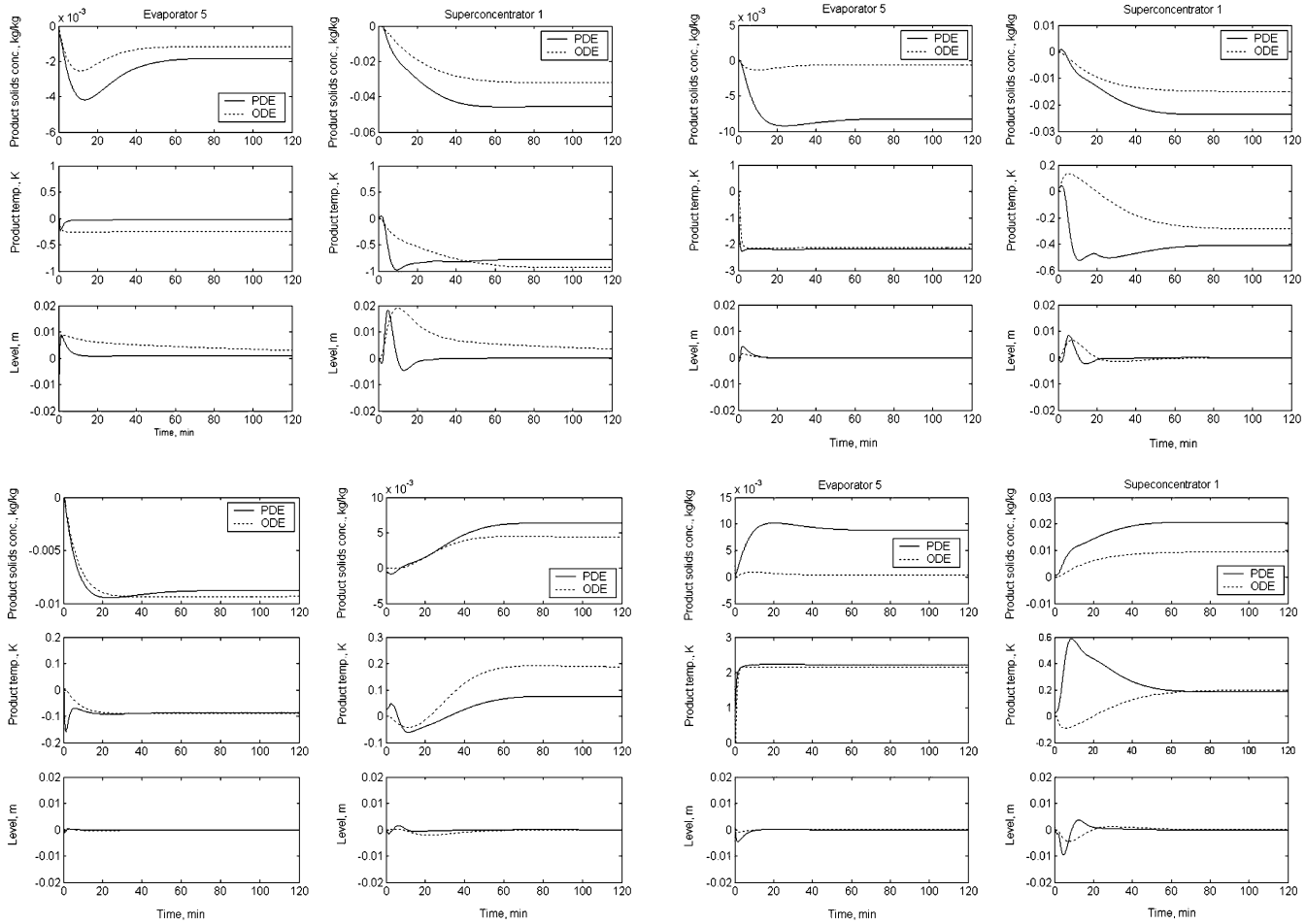

Figure 10. Comparison of the NLPDE and NLODE models. Top left: 5% increase in the feed flow rate. Top right: 5% decrease in the feed temperature. Bottom left: 5% decrease in the feed solids concentration. Bottom right: 5% increase in the feed temperature.

show that the NLODE model is less sensitive to this particular disturbance, especially in the case of evaporator E-5. There are noticeable differences in the profiles of the temperature (T_{prod}) and level (L) responses of the superconcentrator. These differences may be amplified because the parameters of the level controllers of each model are different. Otherwise, it is always possible to tune the level controllers to achieve a closer correspondence. The NLODE model of the evaporator plant will be used to develop a LTI model and, subsequently, a linear MPC.

The LTI state-space model of the evaporator plant is calculated analytically, using Maple. In the development of this linear model, the equation that describes the length of the heating zone is omitted. All levels are assumed constant with a value of 1 m.

The open-loop responses of the linear ODE (LODE) and NLODE models to changes in the input variables, steam pressures, and secondary vapor pressure are shown in Figures 11 and 12. The responses show that the steady-state gains of the LODE and NLODE models are comparable.

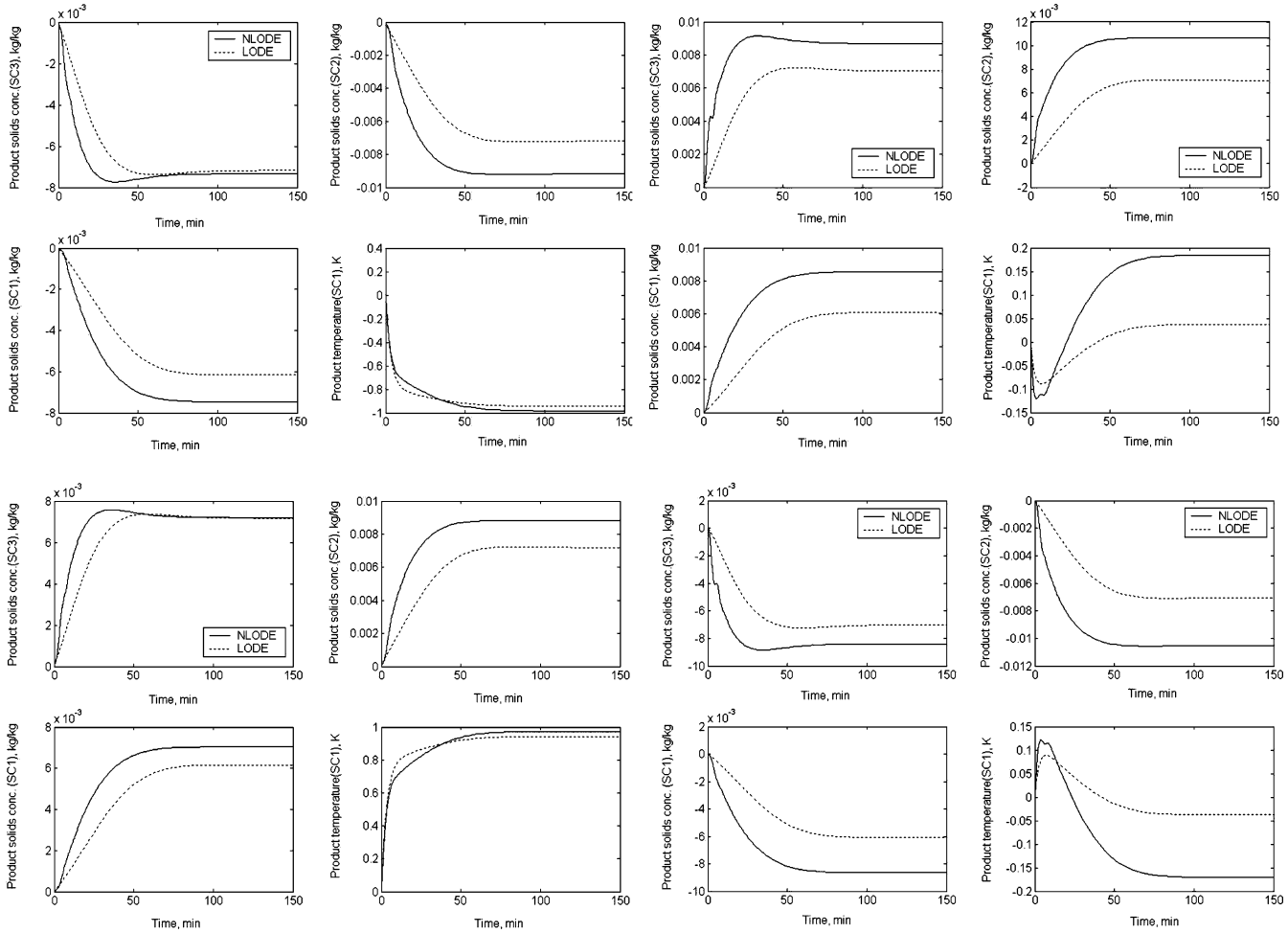

Figure 11. Validation of the LODE and NLODE models of the evaporator plant to changes in the steam pressure. Top left: 5% decrease in the superconcentrator steam pressure. Top right: 5% decrease in the vapor pressure of evaporator E-5. Bottom left: 5% increase in the superconcentrator steam pressures. Bottom right: 5% increase in the vapor pressure of evaporator E-5.

4.2. Linear Model Analysis. A stability analysis of the dynamic constant coefficient matrix (see eq 3) that represents the Jacobian of the states of the system shows that the real part of each eigenvalue is negative; hence, open-loop stability is assured.[11,12] A total of 2 of the 32 eigenvalues are found to be complex numbers, implying some oscillatory behavior in the open-loop responses. However, the magnitude of the imaginary parts of these eigenvalues is very small (on the order of 10^{-4}) when compared to the largest eigenvalue of the system (-2.1465).

The manipulated variables are the steam pressures ($P_{s,j}$) of the superconcentrator (j = SC-1, SC-2, and SC-3) and the secondary vapor pressure (P_{cond}) of evaporator E-5. A linear controllability analysis shows that the system is not state controllable;[12] the rank of the controllability matrix is 4, but the number of states is 32. The measured (controlled) variables of the MEV plant are the solids concentrations in the effluent streams of SC-3, SC-2, and SC-1 and the temperature of the product stream of SC-1. An output controllability analysis shows that the system is output controllable.

4.3. MPC Design. The MEV operates in an *on-supply* mode. Real evaporator plants operate between 0.7 and 0.75 kg/kg solids concentration. The empirical correlations of the black liquor physical properties used in the model by ref 6 were developed for this range. Thus, large deviations outside this range may render the empirical correlations incorrect and/or infeasible. The nominal operating conditions of the MEV plant are provided in Table 3. The MPC design uses prediction and control horizons of 50 and 2.5 min, respectively. The other design parameters are listed in Table 4.

Figures 13 and 14 show the closed-loop performance of the NLODE model of the evaporator plant. The feed mass flow rate is decreased by 5%, and the feed solids concentration and feed temperature are each decreased by 5%. The heat-transfer coefficients (h_E) of the evaporators also are decreased by 10%. The degree of disturbance compensation by the MPC strategy is assessed by the integral of the absolute error (IAE) between the set point (y_{sp}) and the measured value [$y(t)$][7]

$$\mathrm{IAE} = \int_0^T |y_{sp} - y(t)| d \tag{5}$$

Values of the IAE are given in Table 5.

All of the closed-loop responses are stable. There are no offsets in the responses of the controlled variables, and the approach to set point is continuous and without excessive oscillations or discontinuities. Similar descriptions can be stated for the controller actions (manipulated variables).

The closed-loop responses show a greater sensitivity to throughput (feed mass flow rate) changes (see Table 5). The $\pm 1\sigma$ limit on the solids concentration is an active constraint of only the product stream of SC-1. Constraints on the other two product streams' solids con-

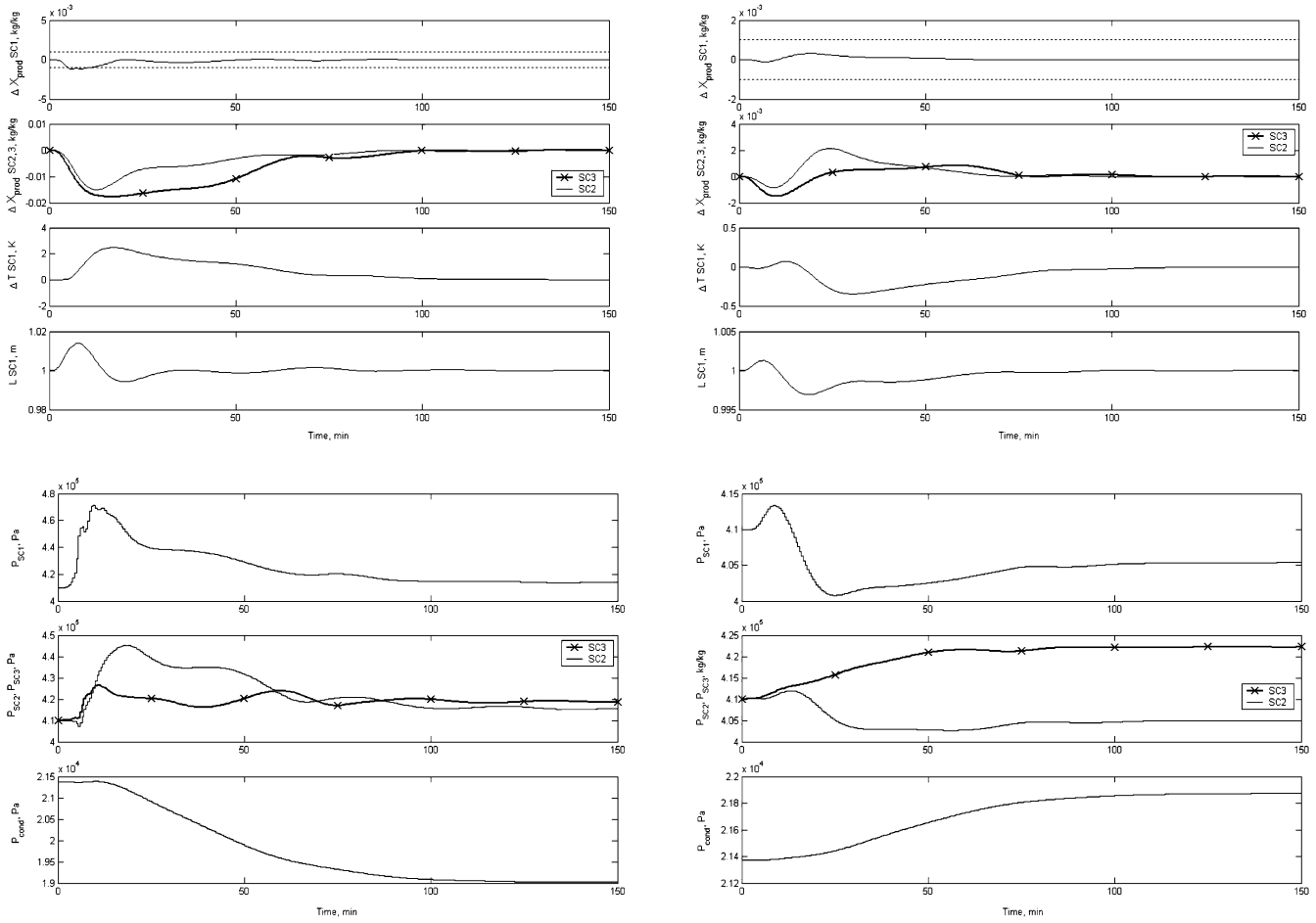

Figure 12. Closed-loop performance of the MPC on the MEV plant. Left: Feed mass flow rate disturbance. Right: Feed solids concentration disturbance.

Table 3. Nominal Operating Conditions of the MEV Plant

parameter	value
G_{feed}	116 kg/s, 50/50 split
X_{feed}	0.145 kg/kg
T_{feed}	303.15 K
$P_{s,j=SC\text{-}1-SC\text{-}3}$	460 kPa
$P_{cond,E\text{-}5}$	21.4 kPa

centrations need not be active because only the product stream of SC-1 is fed to the recovery boiler. The temperature of the product stream of SC-1 is constrained to within ±3 K from the desired set point. The limits on the manipulated variables are selected to satisfy reasonable process limits such as a maximum on steam consumption or a minimum on the secondary vapor pressure at E-5. The rate of change on any manipulated variables is at most 30 kPa/min.

The closed-loop responses to changes in the temperature of the feed and the heat-transfer parameter disturbances are similar. The responses with respect to the feed solids concentration changes are less sensitive when compared to the responses to the other disturbances.

It takes approximately 13 min for the closed-loop responses to be within and remain within $\pm 1\sigma$ for all disturbances, except in the case of the change in the feed solids concentration, where the product stream solids concentration never leaves these limits. Also, it is observed that the effect of a change in the effluent solids concentration of evaporator SC-3 is more significant as compared to that of evaporators SC-2 and SC-1

Table 4. MPC Design Parameters for the MEV Plant

	$X_{SC\text{-}3}$	$X_{SC\text{-}2}$	$X_{SC\text{-}1}$	$T_{SC\text{-}1}$	$P_{s,SC\text{-}3}$	$P_{s,SC\text{-}2}$	$P_{s,SC\text{-}1}$	$P_{cond,E\text{-}5}$
weights	40	40	10^4	0.02	10^{-2}	10^{-6}	10^{-6}	10^{-6}
	$X_{SC\text{-}3,min}$	$X_{SC\text{-}2,min}$	$X_{SC\text{-}1,min}$	$T_{SC\text{-}1,min}$	$X_{SC\text{-}3,max}$	$X_{SC\text{-}2,max}$	$X_{SC\text{-}1,max}$	$T_{SC\text{-}1,max}$
output limits	−0.01 kg/kg	−0.01 kg/kg	−0.001 kg/kg	−1 K	0.01 kg/kg	0.01 kg/kg	0.001 kg/kg	1 K
	$P_{s,SC\text{-}3,min}$	$P_{s,SC\text{-}2,min}$	$P_{s,SC\text{-}1,min}$	$P_{cond,E\text{-}1,min}$	$P_{s,SC\text{-}3,max}$	$P_{s,SC\text{-}2,max}$	$P_{s,SC\text{-}1,max}$	$P_{cond,E\text{-}5,max}$
input limits (kPa)	−5	−200	−200	−200	10	150	150	150
			$\Delta P_{s,SC\text{-}3}$	$\Delta P_{s,SC\text{-}2}$		$\Delta P_{s,SC\text{-}1}$	$\Delta P_{cond,E\text{-}5}$	
max rate of change (kPa)			15	15		15	15	

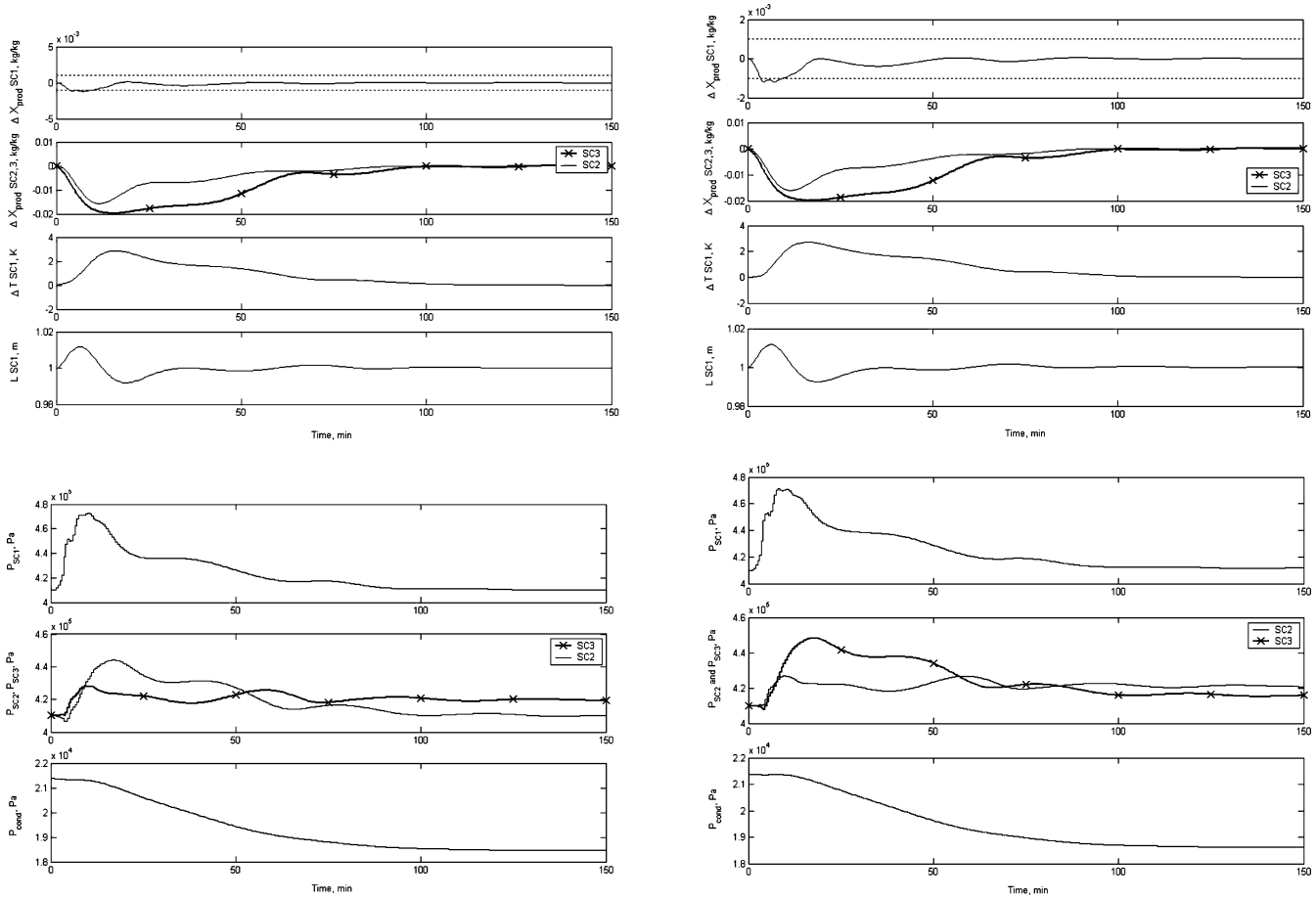

Figure 13. Closed-loop performance of the MPC on the MEV plant. Left: Feed mass flow rate disturbance. Right: Heat-transfer disturbance.

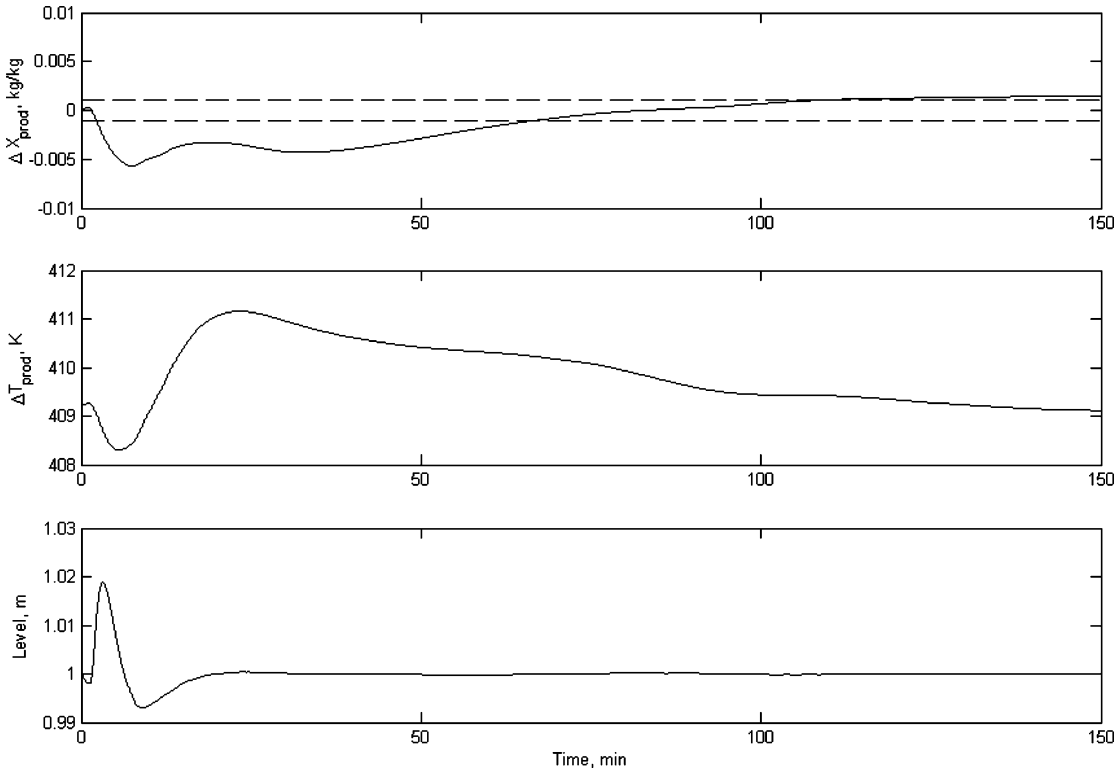

Figure 14. MPC of the nonlinear distributed parameter PDE model of the evaporator plant to a feed flow rate disturbance.

based on the size of the control actions (steam pressure $P_{s,SC\text{-}3}$) acting on SC-3.

Data from a pulp mill operated by Tembec, Inc., show that variations with amplitudes as large as the $\pm 2\sigma$

Table 5. IAE of the Controlled Variables

	controlled variables			
disturbance	$X_{SC\text{-}3}$	$X_{SC\text{-}2}$	$X_{SC\text{-}1}$	$T_{SC\text{-}1}$
$+5\%\ G_{feed}$	1.72	0.88	0.04	203
$-5\%\ X_{feed}$	0.1	0.12	0.016	30
$-5\%\ T_{feed}$	1.77	0.9	0.046	225
$-10\%\ h_E$	2	1	0.046	235

limit do not affect the stability of the recovery boiler. The effect of deviations in this solids concentration range can manifest itself only in the longer term operation of the boiler, where changes in the burning characteristics of the black liquor can be detected.

The results show no constraint violation on the inputs, outputs, and rate of change of the inputs in all cases. The controller actions (a maximum of the rate of change of 30 kPa/min is applied in 1 min or 15 kPa every 30 s, which is the sample time) are more aggressive to compensate for the feed mass flow rate, feed temperature, and heat-transfer disturbances on SC-1.

4.4. MPC of the PDE Model of the Evaporator Plant. Closed-loop control of the PDE system that describes the MEV plant is carried out in the same manner as in the case of a single evaporator (see section 3.3). That is, the manipulated variables found from the control of the NLODE description of the MEV plant are implemented on the PDE system when disturbances in the feed mass flow rate are present. The closed-loop response of the PDE system is shown in Figure 15. The response shows that the MPC actions provide excellent compensation. The solids concentration in the product stream of SC-1 is regulated to within $\pm 1\sigma$ in about 20 min. Also the temperature of the product stream is maintained at the desired set point. Similar observations can be made for other disturbances (feed composition and feed temperature).

5. Summary

A single-loop control scheme and an MPC strategy were developed, tested, and compared on a nonlinear distributed parameter PDE model of a falling-film evaporator. The results showed that both control schemes provided satisfactory disturbance compensation. However, when the magnitudes of the disturbances are increased, the performance of the MPC was found to be superior to that of the PI controllers.

Similar to control of a single evaporator, a constrained MPC formulation was developed and tested on a nonlinear distributed parameter PDE model of a multiple-effect falling-film evaporator plant (seven evaporators). The closed-loop system was subjected to $\pm 5\%$ changes in the feed mass flow rate, feed solids concentration, and feed temperature and 10% parameter uncertainty in the heat-transfer parameters. The feed solids concentration disturbance was well compensated for. In the presence of the other disturbances, the performance of constrained MPC was found to be satisfactory especially in the regulation of the most important variable, the product stream solids concentration of the superconcentrator.

Future work will be directed toward formulating a nonlinear MPC and comparing its performance to that of a linear MPC.

Acknowledgment

Z.S. was supported by Petroleum Research Foundation (Grant 35789-AC9). Both authors are grateful for the data from and discussions with Tembec, Inc. (St. Francisville, LA) and Crestbrook (Cranbrook, British Columbia, Canada).

Appendix: NLODE Model of a Single Evaporator

In the development of the NLODE model of the evaporator, two main sections are considered, the plate stack and the evaporator liquor inventory. In this case, the distributed nature of the transport processes (heating and evaporation) is ignored. The nondistributed model is developed based on the general principles of energy and mass conservation. The detailed model development can be found in ref 6. The final equations are presented here.

The system of ODEs of the plate stack is given by

$$\frac{dM}{dt} = G_{fs} - G_{out} - W \tag{6}$$

$$\frac{dX}{dt} = \frac{G_{fs}}{M}(X_{fs} - X) + \frac{WX}{M} \tag{7}$$

$$W = \frac{h_E a(L - L_h)n[T_{wall} - T_{boil}(X, T_{sat.})]}{\Delta H_{evap}} \tag{8}$$

$$L_h = \frac{G_{fs}c_p(T_{boil} - T_{fs})}{nh_H a\left(T_{wall} - \dfrac{T_{boil} + T_{fs}}{2}\right)} \tag{9}$$

Equation 6 represents the plate stack mass balance, where M is the mass of fluid residing on the plates, G_{fs} is the stack feed mass flow rate, G_{out} is the mass flow rate of the fluid leaving the stack, and W is the mass flow rate of the evaporated water. Equation 7 represents the plate stack solids balance, where X is the solids concentration of the fluid residing on the plates and X_{fs} is the feed solids concentration. Equation 8 is the steady-state energy balance of the plate stack in the case of evaporation, where h_E is the heat-transfer coefficient of evaporation, a is the plate stack width, L is the total plate length, L_h is the length of the plates occupied by a heating zone, n is the total number of plates, T_{wall} is the plate wall temperature, T_{boil} is the fluid boiling temperature, T_{sat} is the saturation temperature at the given vapor pressure, and ΔH_{evap} is the latent heat of evaporation. Equation 9 is the heating zone steady-state energy balance, where c_p is the fluid heat capacity, h_H is the heat-transfer coefficient of sensible heating, and T_{fs} is the feed temperature.

The equations describing the evaporator inventory are

$$\frac{dL_i}{dt} = \frac{nG_p - G_{i,out}}{\rho A_i} - \frac{L_i}{\rho A_i}\frac{d\rho}{dt} \tag{10}$$

$$\frac{dX_i}{dt} = \frac{nG_p}{\rho A_i L_i}(X_p - X_i) \tag{11}$$

$$\frac{dT_i}{dt} = \frac{nG_pT_p - G_{i,out}T_i}{\rho L_r A_i} - \frac{T_i}{\rho}\frac{d\rho}{dt} - \frac{T_i}{L_i}\frac{dL}{dt} - \frac{T_i}{c_p}\frac{dc_p}{dt} \tag{12}$$

Equation 10 represents the bottom inventory mass balance, where L_i is the inventory level, G_p is the mass flow rate of the fluid leaving a single plate, $G_{i,out}$ is the mass flow rate of the fluid that leaves the inventory, ρ

is the density of the fluid in the inventory, and A_i is the inventory cross section. Equation 11 represents the inventory solids balance, where X_p is the solids concentration of the fluid that leaves the plates and X_i is the inventory solids concentration. Equation 12 represents the inventory energy balance, where T_i is the inventory fluid temperature. The correlations for the density and heat capacity of the fluid are analytical functions;[3] the calculation of their derivatives is straightforward.

Literature Cited

(1) Frederick, W. J.; Noopila, T.; Hupa, M. Combustion behavior of black liquor at high solid firing. *Tappi J.* **1991**, *74* (12), 163−170.

(2) Karvinen, R.; Hyoty, P.; Siiskonen, P. The effect of dry solids content on recovery boiler furnace behavior. *Tappi J.* **1991**, *74* (12), 171−177.

(3) Hough, G. *Chemical Recovery in the Alkaline Pulping Processes*, 1st ed.; TAPPI Press: Atlanta, GA, 1985.

(4) Black Liquor Recovery Boiler Advisory Commitee. Safe firing of black liquor in black liquor recovery boilers. www.blrbac.org, Oct 2003. Freely available to the public.

(5) Stefanov, Z. I.; Hoo, K. A. Hierarchical multivariate analysis of cockle. *J. Chemom.* **2003**, *17*, 560−568.

(6) Stefanov, Z. I. Fundamental Modeling and Control of Falling Film Evaporators. Doctor of philosophy, Texas Tech University, Lubbock, TX, 2004.

(7) Seborg, D. E.; Edgar, T. F.; Mellichamp, D. A. *Process Dynamics and Control*, 1st ed.; John Wiley and Sons: New York, 1989.

(8) Camacho, E. F.; Bordons, C. *Model Predicitve Control in the Process Industry*, 1st ed.; Springer-Verlag, New York, 1985.

(9) Stefanov, Z. I.; Hoo, K. A. A Distributed-Parameter Model of Black Liquor Falling Film Evaporators. Part I. Modeling of a Single Plate. *Ind. Eng. Chem. Res.* **2003**, *42*, 1925−1937.

(10) Varma, A.; Morbidelli, M. *Mathematical Methods in Chemical Engineering*; Oxford University Press: New York, 1997.

(11) Rugh, W. J. *Linear System Theory*, 2nd ed.; Prentice Hall: Upper Saddle River, NJ, 1996.

(12) Antsaklis, P. J.; Michel, A. N. *Linear System*; McGraw-Hill: New York, 1997.

(13) Clement, J. L.; Blake, J. W. Economics of high solids black liquor combustion. *TAPPI Engineering Conference*; TAPPI Press: Atlanta, GA, 1996; pp 243−252.

Received for review July 9, 2004
Revised manuscript received January 21, 2005
Accepted January 31, 2005

IE049397W